PERGAMON

International Journal of Heat and Mass Transfer 42 (1999) 2375–2385

International Journal of HEAT and MASS TRANSFER

Investigation of heat transfer characteristics on various kinds of fin-and-tube heat exchangers with interrupted surfaces

J.Y. Yun[a,*], K.S. Lee[b]

[a] *Living System Research Laboratory, LG Electronics Co., Seoul, 153-023, Korea*
[b] *School of Mechanical Engineering, Hanyang University, Seoul, 133-791, Korea*

Received 28 May 1998; in final form 4 September 1998

Abstract

This study experimentally investigates the effects of the shapes of interrupted surfaces on the performance of the fin-and-tube heat exchanger used in home air conditioners. The scaled-up model experiments are conducted to evaluate the heat transfer coefficient and pressure drop, and prototype experiments are also performed to examine the validity of the scaled-up experiments. Their results are in agreement with the available experimental data. These results are confined to the sensible heat transfer characteristics. It is shown that the scaled-up model experiments are very useful for estimating the heat transfer characteristics of a heat exchanger. In this study, the heat transfer and pressure drop characteristics of the three kinds of newly designed fin shapes are also compared to one another, and an optimal fin shape for home air conditioners is recommended.

Nomenclature

A_f fin surface area [m^2]
A_i tube inside surface area [m^2]
A_m tube mean surface area [m^2]
A_o air-side total surface area [m^2]
A_t tube outside surface area [m^2]
C_p specific heat at constant pressure [kJ kg^{-1} K^{-1}]
D_h hydraulic diameter, $D_h = 4\,V_c/A_o$ [m]
f friction factor, dimensionless
FPI fins per inch
G mass flux [kg m^{-2} s^{-1}]
H enthalpy [kJ kg^{-1}]
h heat transfer coefficient [W m^{-2} K^{-1}]
j j factor, dimensionless
k heat conductivity [W m^{-1} K^{-1}]
L heat exchanger depth in air flow direction [m]
M_w water flow rate [kg s^{-1}]
p pressure [Pa]
Δp pressure drop [Pa]
Pr Prandtl number, $Pr = C_p\mu/k$
Q heat transfer rate [W]
R_c thermal contact resistance, [m^2 K W^{-1}]
Re Reynolds number, $Re = VD_h/v$
R_f fouling factor [m^2 K W^{-1}]
ΔT_{am} arithmetic mean temperature difference [K]
T temperature [K]
V air velocity [m s^{-1}]
V_c air-side volume [m^3]
Δx tube thickness [m].

Greek symbols
η surface efficiency
η_f fin efficiency
μ dynamic viscosity [kg m^{-1} s^{-1}]
v kinematic viscosity [m^2 s^{-1}]
ρ air density [kg m^{-3}].

Superscript
* Nondimensional quantity.

Subscripts
a air
ex exit
f fin
h hydraulic
i inside
in inlet

* Corresponding author. Tel.: 0082 2818 3537; fax: 0082 2856 0313; e-mail: jyyun@lge.co.kr

0017–9310/99/$ - see front matter
PII: S0017–9310(98)00310–X

m model
o outside
p prototype
t tube
w tube wall
W water.

1. Introduction

Fin-and-tube exchangers are used extensively in home appliances and transportation applications, where compactness is very important. Fabricating technologies of special shapes, such as a louver or a slit in the fin surface, have been devised to minimize relatively large air-side thermal resistance in fin-and-tube heat exchangers. These efforts have resulted in an increase of the heat transfer coefficient and a reduction in size, and thus the development of compact heat exchangers has been accelerated.

The enhancement of the air-side heat transfer coefficient, in general, can be made using the following three methods [1]: (i) scaling down the geometry [2]; (ii) increasing turbulence; (iii) using interrupted surfaces. Since the use of interrupted surfaces has higher potential for the enhancement of the heat transfer coefficient than the other two methods, it is one of the most widely used techniques. This provides enhancement of heat transfer by the repeated growth and destruction of the laminar boundary layer, the so-called 'leading edge' effect.

Recent studies on heat exchangers have focused on the development of new interrupted surfaces, and so, fin shapes with new design criteria are being suggested. The search for new fin configurations takes much time and effort, hence, experimental studies to analyze the heat transfer characteristics of heat exchangers have not been very active. The geometry similitude method has been employed to alleviate those difficulties in this study, and it has turned out to be effective. Since Wong [3] demonstrated the feasibility of a scaled-up experiment through a comparative study between prototype and the scaled-up model, many researchers have used this method. Torigoe et al. [4] showed experimental results of four scaled-up models with tube diameters of 6.25, 5.0 and 4.0 mm each and three different kinds of step and row pitches to examine the effects of tube diameter and tube arrangement on the heat transfer performance. Koido et al. [5] performed flow visualization tests and numerical analysis using 20 scaled-up heat exchangers with slitted fins to investigate the temperature and velocity field, and selected optimal fin shapes.

In this study, air-side heat transfer characteristics such as the heat transfer coefficient and pressure drop are experimentally analyzed using fin-and-tube heat exchangers with 2-row, staggered arrangements. The geometry similitude experiment using three scaled-up models with three kinds of interrupted fins and a plate fin is conducted in the present study, and the heat transfer coefficient and pressure drop of these fins are measured by utilizing a small-sized wind tunnel. Prototype experiments with these fins are done to verify the scaled-up experiments. By comparing their performance characteristics with the three kinds of fin shapes, the optimal shapes are selected for application to home air conditioners. This work also suggests a process for the development of a new heat exchanger.

2. Performance evaluation procedure

2.1. Scaled-up experiment [6]

2.1.1. Theoretical analysis

The nondimensional governing equations of steady, incompressible flows can be written as follows:

$$\nabla^* \cdot \mathrm{v}^* = 0 \tag{1}$$

$$(\mathrm{v}^* \cdot \nabla^*)\mathrm{v}^* = -\nabla^* p^* + \left(\frac{1}{Re}\right)\nabla^{*2}\,\mathrm{v}^* \tag{2}$$

$$\mathrm{v}^*(\nabla^* \cdot T^*) = \left(\frac{1}{Re\,Pr}\right)\nabla^{*2} T^* \tag{3}$$

where

$$\mathrm{x}^* = \frac{\mathrm{x}}{D_\mathrm{h}}, \quad \mathrm{v}^* = \frac{\mathrm{v}}{V}, \quad \nabla^* = D_\mathrm{h}\nabla,$$

$$p^* = \frac{p - p_0}{\rho V^2}, \quad T^* = \frac{T_\mathrm{w} - T}{T_\mathrm{w} - T_\mathrm{in}},$$

$$Re = \frac{VD_\mathrm{h}}{v}, \quad Pr = \frac{C_\mathrm{p}\mu}{k}, \quad D_\mathrm{h} = \frac{4V_\mathrm{c}}{A_\mathrm{o}} \tag{4}$$

Similitude of the flow field is obtained as the Reynolds number in equation (2) set to be equal value. Similitude of air temperature is also required to obtain similitude of heat transfer. Similitude of fin surface temperature has to be met with the Reynolds and Prandtl numbers in energy equation (3). In this study, similarity of the Prandtl number is automatically satisfied since the working fluid is air. Similitude of fin surface temperature is obtained from the heat conduction equation inside the fin as follows:

$$\nabla^*(k_\mathrm{f}^* \nabla^* T_\mathrm{f}^*) = 0$$

where

$$T_\mathrm{f}^* = \frac{T_\mathrm{f} - T_\mathrm{in}}{T_\mathrm{w} - T_\mathrm{in}}, \quad k_\mathrm{f}^* = \frac{k_\mathrm{f,m}}{k_\mathrm{f,p}} \tag{5}$$

T_f^* and k_f^* represent dimensionless fin temperature and thermal conductivity, respectively. Since fin thickness and thermal conductivity must have the same values as those of the prototypes in order to have similarity for fin surface temperature, fin thickness may be scaled-up as much as the scale factor.

2.1.2. Experimental apparatus and procedure

Figure 1 shows the schematic diagram of the experimental apparatus which is an open type, small-sized wind tunnel [7]. It consists of a suction fan, flow straightener, first reduction area, a test section, second reduction area, and exit chamber. The air flow rate and velocity are determined by using the measured pressure difference at the nozzle installed inside the exit chamber. The pressures at eight pressure taps are measured by a micro-manometer with resolution of 0.1 Pa and the average pressure difference is determined from these data. The air flow rate is calibrated by a pitot tube at the downstream of nozzle and the deviation between these two data is within 0.3%. The air velocity is varied from 0.2 to 1.0 m s^{-1} using a fan connected to the power regulator. Static pressure is measured using six pressure taps which are installed at the inlet and the outlet of the test section. Pressure drop is measured using a differential pressure gauge. Average temperature difference of air is measured using type T thermocouple installed at the same positions. To control the inlet temperature with the same conditions as the actual product, an air-cooled heat exchanger with a water tank at constant temperature is placed at the inlet section of the chamber. The outlet temperature is estimated by averaging the temperatures at two locations in exit chamber. Styrofoam of 40 mm thickness is used to minimize the heat loss.

The test section is composed of nine fins and eight rings that correspond to the tube in the prototype. To maintain the wall temperature under the same condition as that of the actual product, the rings are heated by Joule heating. Electric power on the front and back rows can be controlled independently for the convenience of heat transfer calculation. Aluminium fins and tubes are screwed tightly to minimize contact resistance. Tube wall temperature is measured using type T thermocouples.

The experiment starts with supplying electricity to the heating wire after fan speed reaches the maximum value. The amount of electric power is measured after the wall temperature reaches a steady state at every measuring point. The steady state is generally obtained in 30 min, and the test is repeated with increasing or decreasing velocity to identify the reproducibility. The heat transfer coefficient is obtained as follows:

$$h = \frac{Q}{A_o \Delta T_{am}} \tag{6}$$

where

$$\Delta T_{am} = T_w - \frac{(T_{ex} + T_{in})}{2} \tag{7}$$

Q and ΔT_{am} represent the amount of power supplied and the arithmetic mean temperature difference, respectively. All the temperature measurements with the thermocouples are made with an uncertainty of $\pm 0.1^{\circ}$C.

2.2. Prototype experiment

The prototype experiment is performed to confirm the validity of the geometry similitude experiment. Samples are made to actual size using a fin die, and their heat transfer and pressure drop characteristics are measured at the open-type wind tunnel inside a psychrometric type

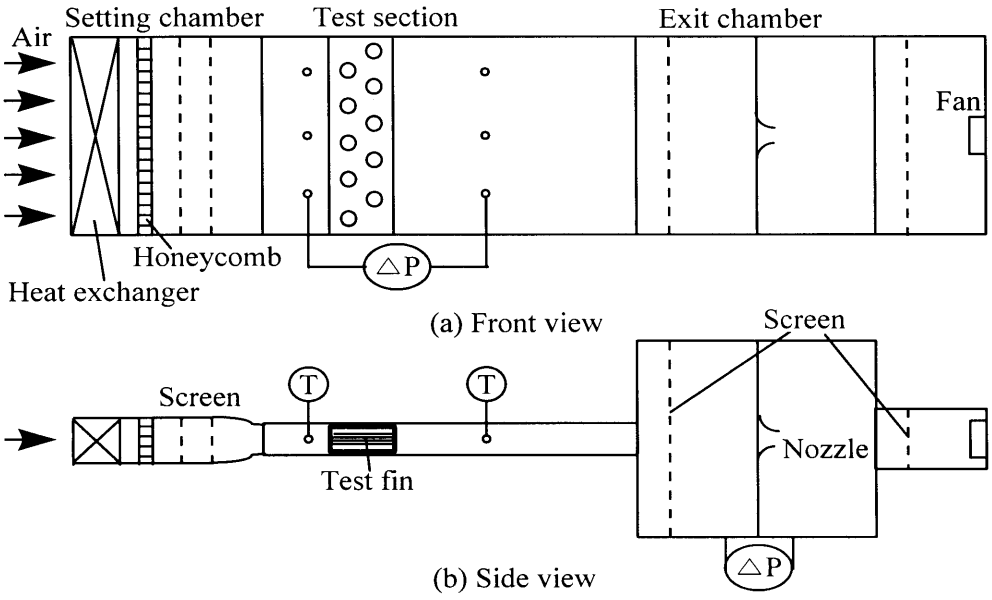

Fig. 1. Schematic diagram of the test apparatus for scaled-up experiment.

calorimeter which has similar principles to the scaled-up experimental apparatus. This unit is composed of a test section, a control chamber, cooling equipment, a blower section, hot and cold water supply unit, and a refrigerant supply unit. The accuracy and test conditions of this unit are shown in Table 1. This experiment has been performed to measure only the sensible heat transfer characteristics using hot water to compare it with the scaled-up experimental results under the same conditions. The acceptance criteria of the prototype experimental data are judged by the heat balance ratio of air-to-water under the steady state condition, which is available in the ASHRAE Standard 33-78 [8]. An overall error of less than $\pm 4\%$ in the heat balance is permitted in this study. Since the present results satisfy the heat balance and the data reading under the steady state, these experiments are considered as a 'valid' run. This balance is automatically calculated utilizing the data acquisition and reduction program. The steady state is obtained between 30 and 60 min at every measuring point. The heat transfer rate in the tube-side and air-side is obtained using the inlet and outlet temperature and enthalpy, respectively, which can be expressed as follows:

$$Q_{\mathrm{W}} = M_{\mathrm{W}} C_{\mathrm{pW}} (T_{\mathrm{Wi}} - T_{\mathrm{Wo}}) \tag{8}$$

$$Q_{\mathrm{a}} = G_{\mathrm{a}} (H_{\mathrm{ao}} - H_{\mathrm{ai}}) \tag{9}$$

The subscripts Wi, Wo, ai and ao denote the water inlet, the water outlet, the air inlet and the air outlet, respectively. The air-side heat transfer coefficient is calculated using a modified Wilson plot method [9]:

$$Q = FUA_{\mathrm{o}} \Delta T_{\mathrm{am}} \tag{10}$$

where F represents the correction factor, and Q is obtained from the arithmetic mean of equation (8) and (9). Since water flow rate is increased with maximum possible rate to minimize the temperature difference between the inlet and outlet and the arithmetic mean temperature difference is used in the calculation process, the value of F is assumed to be unity. The overall heat transfer coefficient U is expressed by

$$\frac{1}{U} = \frac{1}{h_{\mathrm{o}}} + R_{\mathrm{f}} + R_{\mathrm{c}} + \frac{\Delta x}{A_{\mathrm{m}} k_{\mathrm{t}} / A_o} + \frac{A_{\mathrm{o}}}{A_{\mathrm{i}} h_{\mathrm{i}}} \tag{11}$$

where

$$h_{\mathrm{o}} = \eta h = \frac{(A_{\mathrm{t}} + \eta_{\mathrm{f}} A_{\mathrm{f}})}{A_{\mathrm{o}}} h, \quad h_{\mathrm{i}} = 0.023 Re^{0.8} Pr^{0.4} \frac{k}{d_{\mathrm{i}}} \tag{12}$$

Since the heat exchangers of the same size are used in this study, the second to fourth terms of the right hand side in equation (11) can be treated as constants. In equation (12), h represents the pure heat transfer coefficient of the tube outside at the 100% fin efficiency, η_{f}. Since the fin efficiency is difficult to be obtained experimentally, the heat transfer coefficient including the effect of fin efficiency is adopted in the present study. Consequently, the air-side heat transfer coefficient h_{o} is determined using the overall heat transfer coefficient U of equation (10) and the tube side heat transfer coefficient h_{i} of equation (12). Colburn j factor and friction factor are, respectively, given by

$$j = \frac{h_{\mathrm{o}} Pr^{2/3}}{\rho C_{\mathrm{p}} V} \tag{13}$$

$$f = \frac{D_{\mathrm{h}}}{L} \frac{2\Delta p}{\rho V^2} \tag{14}$$

where ρ and C_{p} represent air density and specific heat at constant pressure, respectively.

3. Experimental model

The basic model in this work is chosen as the heat exchanger with a 2-row, staggered arrangement and tube diameter of 7 mm, which is extensively used in room air conditioners. A scale factor is selected by considering the manufacturing process of the sample and measuring accuracy. In the case of a three scaled-up model, all geometries have to be enlarged to three times the prototype. Table 2 shows geometric configurations of the samples. In the present scaled-up procedure, the heat transfer coefficient and the pressure drop must be one third and one ninth, respectively, of the actual value to satisfy the similarity with the prototype as shown in Table 3.

Figure 2 represents five kinds of fin shapes used in the present work. Type 'R' fin is a standard fin for comparisons of validity, and a leading edge effect is maximized by being formed by cutting the metal plate and

Table 1
Accuracy and test conditions of psychrometric type calorimeter

Physical parameter	Accuracy	Physical parameter	Test condition
Temperature (°C)	±0.1	Air dry bulb temperature (°C)	21
Pressure (Pa)	±0.1	Air wet bulb temperature (°C)	15.5
Air flow rate ($m^3\ min^{-1}$)	±0.1	Air velocity ($m\ s^{-1}$)	0.5 ~ 1.5
Water flow rate ($kg\ h^{-1}$)	±0.6	Inlet water temperature (°C)	45

Table 2
Basic geometries on experimental heat exchanger

Geometric parameter	Scaled-up model	Prototype model
Scale factor	3	1
Frontal area (mm^2)	36×315	290×231
Tube diameter (mm)	22.5	7.5
Fin pitch (mm)	3.6	1.2
Fin thickness (mm)	0.3	0.1
Row pitch (mm)	38.1	12.7
Step pitch (mm)	63	21
Number of rows	2	2
Number of steps	5	11
Hydraulic diameter (mm)	6.3	2.1

Table 3
Comparison of similitude relations on parameters used in this study

Geometric parameters	Scaled-up model	Prototype model
Scale factor	3	1
Fin length (mm)	3	1
Fin thermal conductivity ($W\,m^{-1}\,K^{-1}$)	1	1
Fin thickness (mm)	3	1
Fin surface temperature (K)	T(x, y)	T(x, y)
Air velocity ($m\,s^{-1}$)	1/3	1
Heat transfer rate (W)	3	1
Heat transfer coefficient ($W\,m^{-2}\,K^{-1}$)	1/3	1
Pressure drop (Pa)	1/9	1
Re, *Pr* number	1	1
j, *f* factor	1	1

raising the cut elements to both sides alternatively. It has a X shape when viewed from the front. Experimental results on these shapes are already reported in the literature [10]. Type 'SA' fin is a kind of slitted fin and is designed to promote convective heat transfer from the tube-side by allowing more air over the tube. The slitted structure is similar to the type 'R' fin. Although the type 'R' fin is formed at an angle of 50° with slit forming surfaces based on a center line connected between tubes, this fin is formed at 80°. This also reduces pressure drop by decreasing the allowable forming area of interrupted surfaces. Type 'SB' fin is also a kind of slitted fin and is designed to induce the turbulence of inflow air and the uniform velocity of outflow air as the slits of the inlet and outlet sections are cut into three parts [11]. The four array slit group in the central section is formed with a simple rectangular shaped slit to conform to the air flow direction. Slitted fins are made up of six array slits. Type 'L' fin is a kind of parallel louvered fin and is used to compare heat transfer with the slitted fins. This is designed for use in home air conditioners operated under a relatively low velocity by reducing the number of multi louvers to three couples, which has been used mainly in high velocity flow such as automotive air conditioners. Type 'P' fin is a plate fin. Three fins, except type 'R' and 'P' fins, are designed in this study.

4. Results and discussion

In this study, air-side heat transfer characteristics are analyzed using five different kinds of fin-and-tube heat exchangers, and the scaled-up experiment is conducted for this purpose. These results are compared with experimental results using the prototype to confirm its availability as a development tool for a new heat exchanger. The results of Hiroaki on the type 'R' fin are used to verify the validity of the scaled-up experiment. The heat transfer coefficient and pressure drop on both experiments are measured by varying the air velocity at the test section. The heat transfer coefficient and pressure drop in the scaled-up model should be converted to the actual value to compare with them in the prototype model. A conversion to the actual value from the scaled-up experimental results can be obtained by multiplying the heat transfer coefficient and velocity by three and multiplying pressure drop by nine. They are marked with actual values in all figures.

4.1. Verification of scaled-up experiment

Figures 3 and 4 show the heat transfer coefficient and pressure drop of the scaled-up model and the prototype model with respect to air velocity for the type 'R' fin. The data from the scaled-up model is enlarged three times. Hiroaki's result on the heat transfer coefficient is also obtained using the modified Wilson-plot method. The heat transfer coefficient on the scaled-up model shows relatively good agreement with the prototype results at an air velocity of about 1.0 $m\,s^{-1}$, but it is underestimated by 2.7% at the velocity of 1.5 $m\,s^{-1}$. Considering that the performance estimation on the prototype generally has a measurement error of 3.0%, the present scaled-up model predicts the heat transfer characteristics of the prototype very well. The uncertainty of the heat transfer coefficient on the scaled-up experiment is 3.6–4.0% according to the velocity range.

It is shown that the pressure drop in the prototype experiment is higher by approximately 3.2% than that of the scaled-up experiment at the velocity of 1.0 $m\,s^{-1}$. However, the two results are in good agreement at the velocity of over 1.5 $m\,s^{-1}$. The uncertainty of pressure drop on the scaled-up experiment was 2.8–5.0% accord-

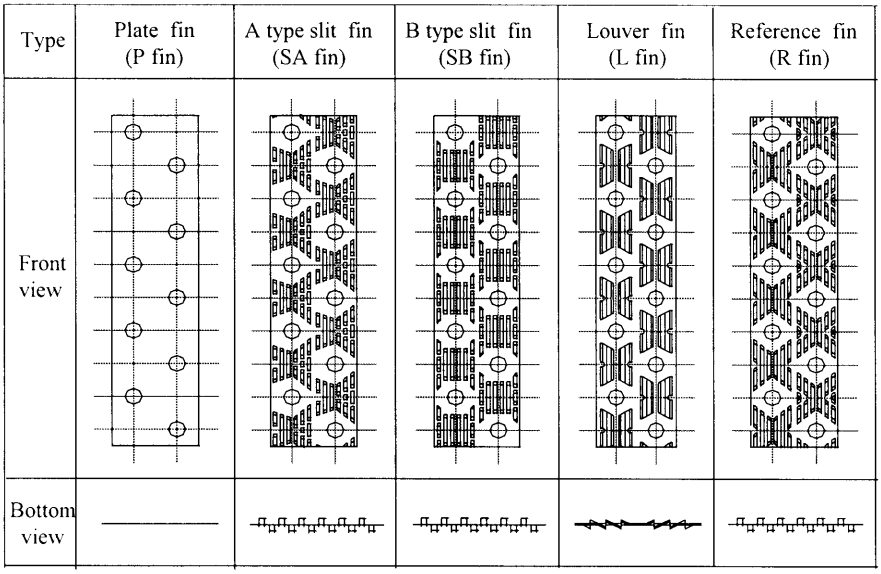

Fig. 2. Five kinds of fin shapes used in this study.

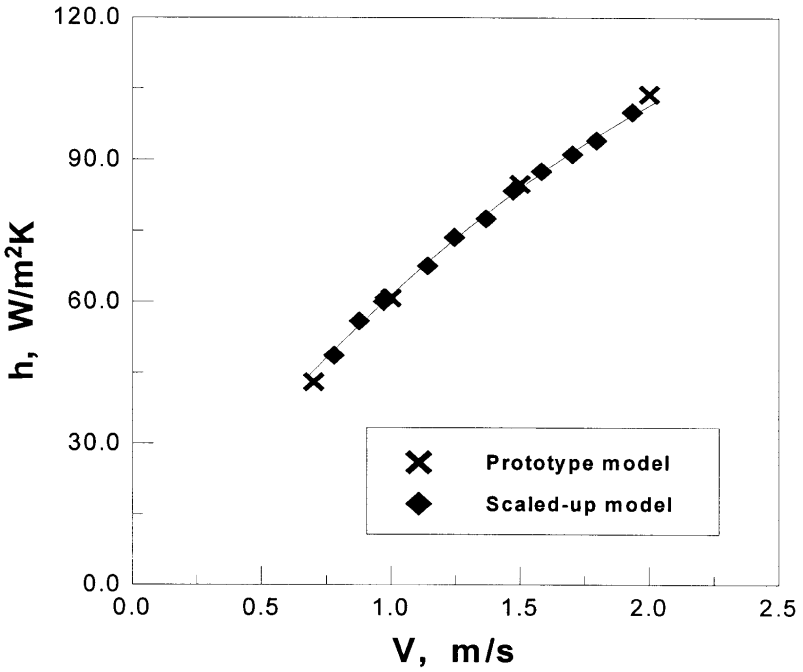

Fig. 3. Comparison of the heat transfer coefficients for scaled-up and prototype models using type 'R' fin.

ing to the velocity range. Since pressure drop of a resisting body is proportional to the square of velocity, the scaled-up model results fitted to a quadratic curve can be closer to the actual state compared to the prototype results. Hence, a scaled-up model can predict the heat transfer coefficient and pressure drop more accurately. These

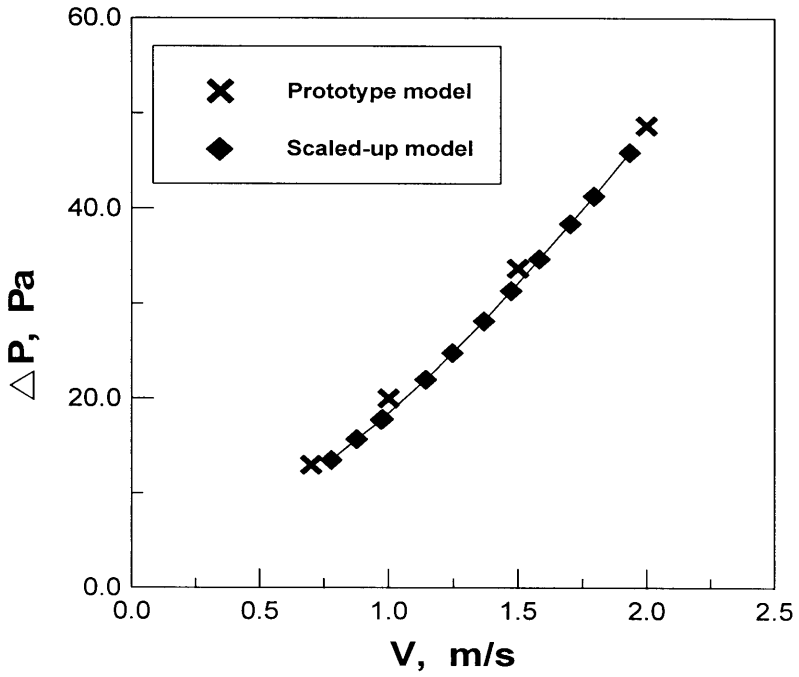

Fig. 4. Comparison of the pressure drop for scaled-up and prototype models using type 'R' fin.

results can also be used effectively in the development of a new heat exchanger.

4.2. Comparison of heat transfer characteristics

4.2.1. Interrupted fins

Figures 5–7 show the heat transfer coefficient and pressure drop of the scaled-up model and the prototype model, respectively, with respect to air velocity for type 'SA', 'SB' and 'L' fins.

As far as the type 'SA' fin is concerned, the heat transfer coefficient of the prototype is higher by approximately 2.3% than that of the scaled-up model at the velocity of 1.0 m s^{-1}. However, the two results are in good agreement at the velocity of 1.5 m s^{-1}. The value of the heat transfer coefficient on this type fin is about 63 W m^{-2} K^{-1} at the velocity of 1.0 m s^{-1}, and is approximately the same as that of the type 'R' fin which is about 65 W m^{-2} K^{-1} at the same velocity. This indicates that a minute change of a slitted area shows little influence on heat transfer enhancement in the fin-and-tube heat exchangers. It is shown that the heat transfer coefficient can also be predicted accurately using a scaled-up experiment. The pressure drop of the prototype model is higher by about 9.5–16.5% in comparison to that of the scaled-up model with increasing velocity.

The heat transfer coefficient of the prototype model on a type 'SB' fin shows a higher value by about 4% than that of the scaled-up model at the velocity of 1.0 m s^{-1}, but it is overestimated by approximately 4.6% at the velocity of 1.5 m s^{-1}. Since the value of the heat transfer coefficient is nearly the same as that of the type 'SA' fin, it is clear that slitted fins have little effect on the variation of pattern. The pressure drop of the prototype model on this type of fin is higher by about 16–18% compared with that of the scaled-up model with increasing velocity. It is expected from this result that the slit pattern formed on the fin surface has a substantial influence on the pressure drop of slitted fins.

The heat transfer coefficient of the prototype model on the type 'L' fin shows good agreement with that of the scaled-up model within $\pm 2\%$ error for the overall velocity ranges. This is the lowest among the fins considered in this work. The pressure drop of the prototype model on this type fin is about 23% higher than that of the scaled-up model for overall ranges. Compared to the slitted fins, the type 'L' fin has yielded the slightly large deviation between the pressure drop in the prototype and that in the scaled-up model. This may be attributed to the following: the flow pattern in the slitted fin is parallel to the wall of wind tunnel, but the louvered fin shows a slanted flow pattern. The effect of flow pattern is negligible in the prototype with many fins. However, it might be possible that the pressure drop in the scaled-up exper-

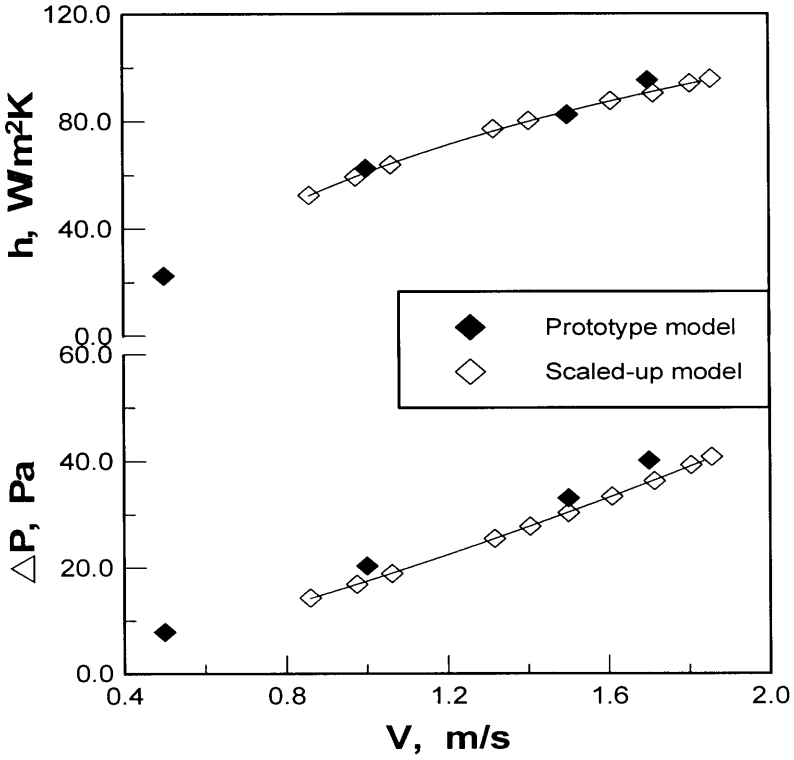

Fig. 5. Heat transfer coefficient and pressure drop characteristics of type 'SA' fin.

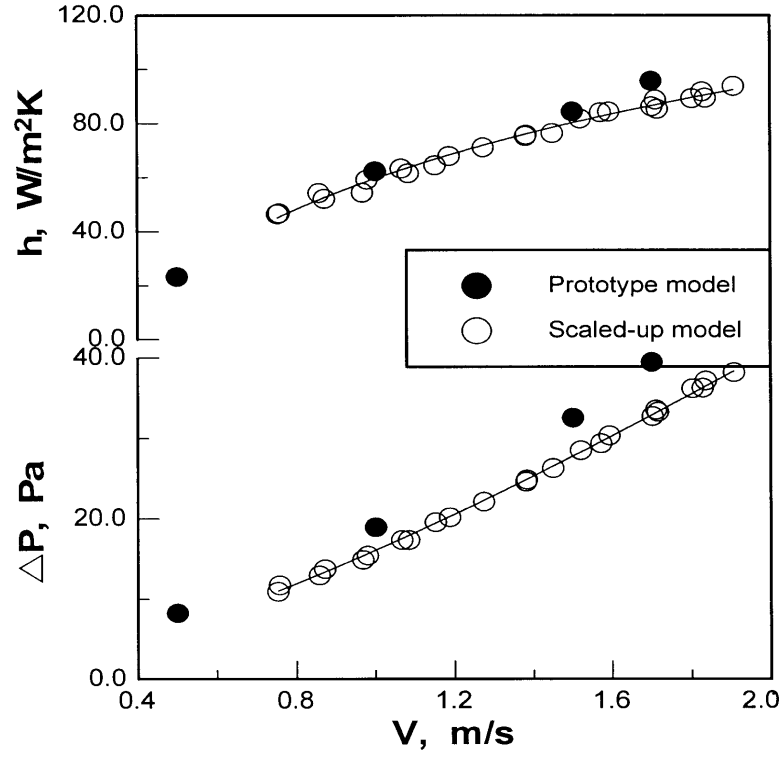

Fig. 6. Heat transfer coefficient and pressure drop characteristics of type 'SB' fin.

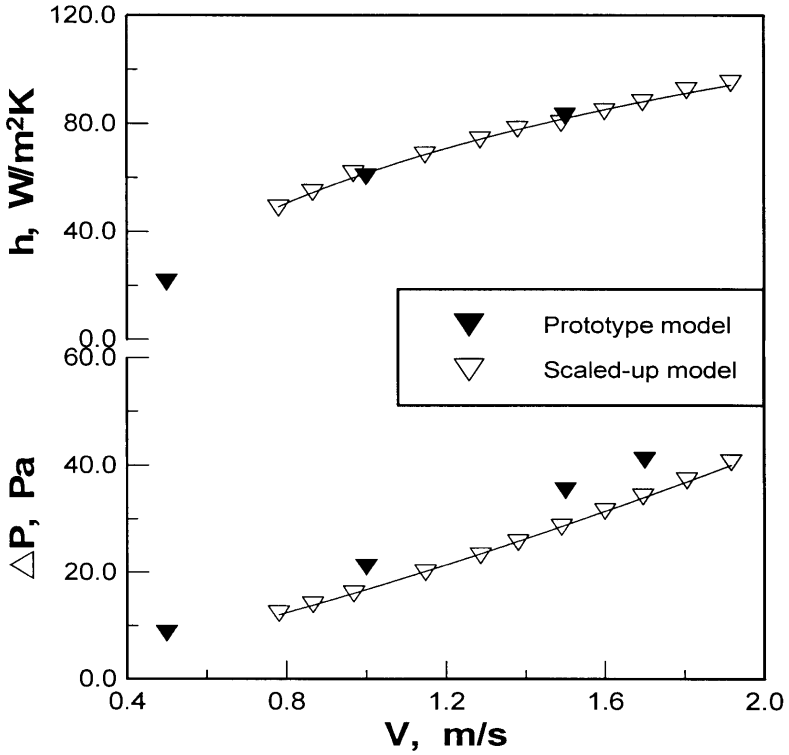

Fig. 7. Heat transfer coefficient and pressure drop characteristics of type 'L' fin.

iment using 10 fins could be slightly affected due to the difference of flow characteristics.

4.2.2. Plate fin

Figure 8 shows the heat transfer coefficient and pressure drop of the scaled-up model and the prototype model with respect to air velocity for a plate fin. The heat transfer coefficient of the prototype model is almost the same as that of the scaled-up model at the velocity of 1.0 m s^{-1}, however, it is higher by about 4.5% at the velocity of 1.5 m s^{-1}. The heat transfer coefficient of plate fin shows a little different trend with that of interrupted fins. It is believed that this is due to the fact that the thermal boundary layer of plate fin has a different growth process with that of interrupted fins. Therefore, it is expected that the more accurate data on the heat transfer coefficient may be obtained by using the l-row heat exchanger sample or reducing the scale factor. The heat transfer coefficient of the prototype model is higher by about 19–25% in comparison to that of Webb's correlation [12] with increasing velocity. It is shown that some deviation between the two results exists, since Webb's correlation has been proposed at a higher velocity region compared to the present experimental condition. It is measured when the FPI of the heat exchanger is less than 21. However, the difference is very small, and the characteristics between the two results have similar tendencies.

The pressure drop of the prototype model is higher by about 22–14.6% in comparison to that of the scaled-up model with increasing velocity.

It is shown that performance is possible to predict using the present result, although it depends greatly on the suitability of the scaled-up experimental apparatus on plate fin and the measurement accuracy at the low velocity. As shown above, the scaled-up experimental apparatus in this study can predict the results very well in the case of the interrupted surface fins, but careful evaluation of experimental procedure must be considered for accurate measurement for plate fin.

4.2.3. Comparison of j *and* f *factors*

Figure 9 shows the variations of j and f factors on the prototype model with respect to the Reynolds number for four kinds of fin shapes. Note that the data on the Reynolds number below 100 are not presented in this figure, although the experiment has been performed at the velocity of 0.5 m s^{-1}, corresponding to the Reynolds number of 61. This is due to the fact that natural convection is dominant if the Reynolds number is below 100. In such cases, unreasonable results may be obtained since

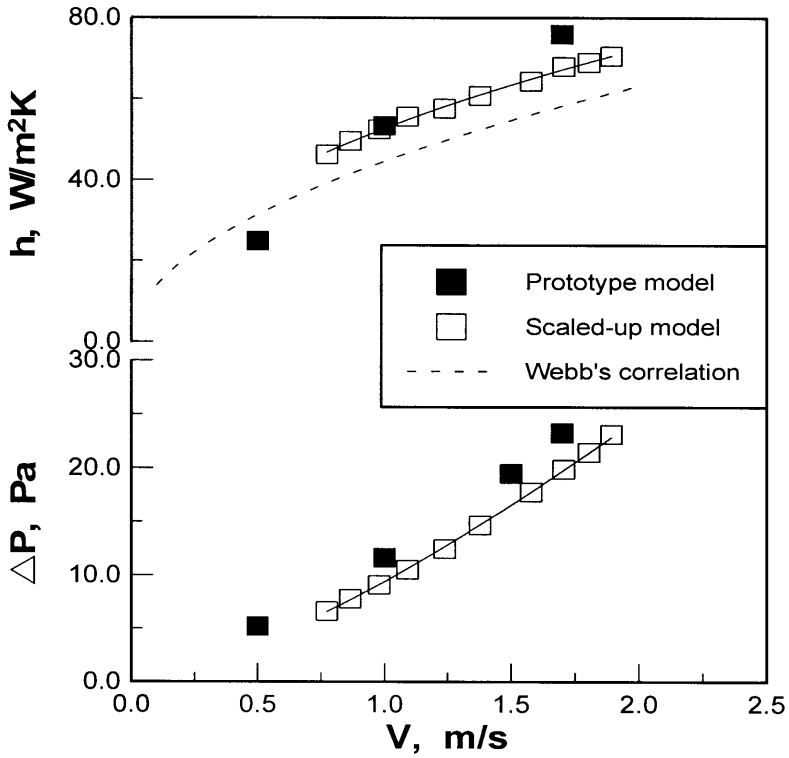

Fig. 8. Heat transfer coefficient and pressure drop characteristics of plate fin.

heat exchangers are generally operated under forced convection. Therefore, the results in this figure are limited to the operating range of home air conditioners. The results show that the magnitude of the j factor is in the order of SB, SA, L and P fins, and the f factor shows in the order of L, SA, SB and P fins. The j factors of the type 'SA' and 'SB' fins are almost the same, however the f factor of the type 'SB' fin is less than that of the 'SA' fin. The thermal performance of the type 'SB' fin is relatively better than that of the other fins when considering only sensible heat transfer performance, and it is also shown that the type 'SB' fin has the lowest pressure drop. The results displayed in Fig. 9 suggest that the heat transfer characteristics of the type 'SB' fin is superior to that of the 'SA' fin in the Reynolds number of over 200, although there is little difference between them. It is believed that this phenomenon at a relatively high velocity is due to the increase of turbulent flow, resulting from the fact that the slits of the inlet and outlet section are divided into three parts. Hence, the type 'SB' fin shows superior characteristics in the view of heat transfer and pressure drop when it is applied to an actual design. However, this is in contrast to the case of the type 'L' fin, where there is little difference in thermal performance among the interrupted surface fins over the ranges of the Reynolds number considered in the present work. Therefore, any type of fin is applicable to home air conditioners. Since the f factor of the type 'SA' fin is approximately the same as that of the type 'SB' fin with increasing velocity, it is shown that the slitted fins with 6 array have similar flow resistance. However, the f factor of the louvered fin is relatively higher than that of the slitted fins over all ranges, hence, it is not good in view of the heat transfer and the pressure drop characteristics.

5. Conclusions

This study presents heat transfer characteristics according to fin shapes in fin-and-tube heat exchangers. The scaled-up and prototype experiments have been performed to analyze the characteristics of heat transfer coefficient and pressure drop for each fin. The conclusions from the present work are as follows:

(1) The heat transfer and pressure drop characteristics of the scaled-up model on the type 'R' fin show good agreement with those of Hiroaki's prototype within an error of 3% over all ranges of operating velocity. The heat transfer coefficient from the scaled-up experiment for the proposed interrupted fins predicts an actual value within an error of 4.5%; however,

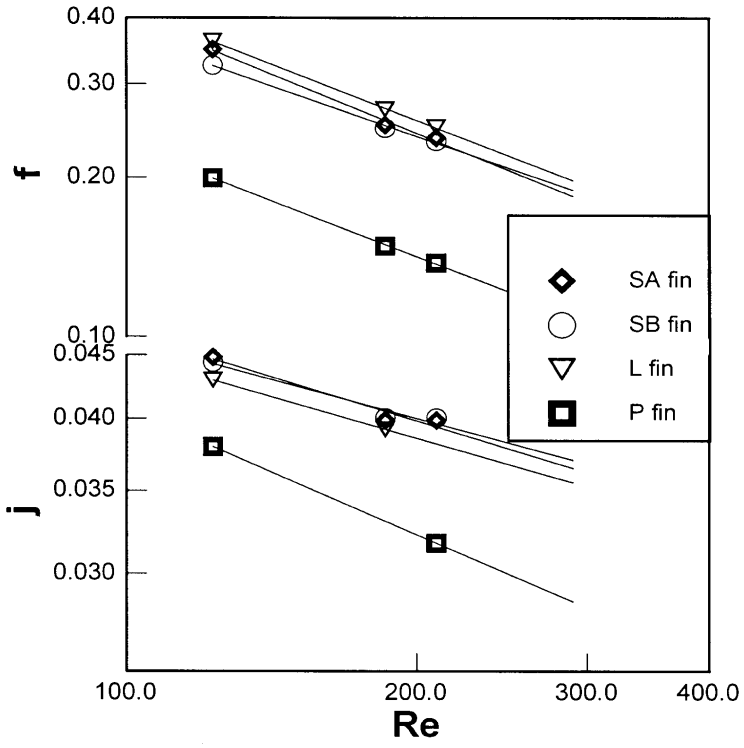

Fig. 9. *j*, *f* factor vs Reynolds number in the prototype model.

the pressure drop decreases by about 10–23% compared to the prototype, irrespective of fin shapes. Although there is a large deviation in the pressure drop, it is believed that the present result is reliable since it shows a similar trend. Consequently, it is confirmed that these tools may be very helpful in the development of a new heat exchanger.

(2) It is indicated that all of the proposed interrupted fins have suitable characteristics for home air conditioners, and the deviations in the heat transfer and pressure drop performance between them are also very small. However, the type 'SB' fin, of the three kinds of interrupted fins, is recommended as an optimal shape.

References

[1] C. Marvillet, Recent development in finned tube heat exchanger theoretical and practical aspects, DTI, Energy Tech. Denmark, (1993) 91–159.

[2] K. Torikoshi, K. Kawabata, H. Yamashita, K. Yasuao, Heat transfer performance of mesh fin type air-cooled heat exchanger, Proceedings of Symposium of Heat Transfer Soc. of Japan, 1992, pp. 539–540.

[3] L.T. Wong, M.C. Smith, Air flow phenomena in the louvered fin heat exchanger, S.A.E., Paper No. 730237, 1973.

[4] K. Torikoe, et al., Heat transfer characteristics on fin-and-tube type heat exchanger, Proceedings of 27th JAR Annual Conference, 1993, pp. 109–112.

[5] T. Koido, et al., Development of compact heat exchanger for air conditioner, Proceedings of 26th JAR Annual Conference, 1992, pp. 165–168.

[6] J.Y. Yun, K.S. Lee, Heat transfer characteristics of fin-and-tube heat exchangers with various interrupted surfaces for air-conditioning application, Transactions of KSME 20 (1996) 3938–3948.

[7] W.H. Rae Jr., A. Pope, Low Speed Wind Tunnel Testing, 2nd ed., John Wiley & Sons, Inc., 1984.

[8] ASHRAE STANDARD 33–78, Methods of Testing Forced Circulation Air Cooling and Air Heating Coils, ASHRAE, Inc., 1978.

[9] H.F. Khartabil, R.N. Christensen, D.E. Richards, A modified wilson plot technique for determining heat transfer correlations, 2nd U.K. National Conference on Heat Transfer, September 1989.

[10] K. Hiroaki, I. Shinichi, A. Osamu, K. Osao, High efficiency heat exchanger, National Technical Report 35 (1989) 71–79.

[11] S. Takashi, S. Kiyoshi, A. Masahiro, T. Teruhiko, K. Takumi, O. Hironari, Low noise fan for air conditioners, National Technical Report 35 (1989) 94–100.

[12] D.L. Gray, R.L. Webb, Heat transfer and friction correlations for plate fin-and-tube heat exchangers having plain fins, Proceedings of 9th Int. Heat Transfer Conf., San Francisco, 1986.